IEEE Access
Multidisciplinary ⋮ Rapid Review ⋮ Open Access Journal

Received 24 December 2023, accepted 26 January 2024, date of publication 6 February 2024, date of current version 13 February 2024.

Digital Object Identifier 10.1109/ACCESS.2024.3363229

RESEARCH ARTICLE

Offshore Oilfield Inspection Planning With Drone Routing Optimization

HAOYAN ZHANG
College of Marine Engineering, Dalian Maritime University, Dalian 116026, China
e-mail: zhanghy_orc@163.com

ABSTRACT Offshore oilfield inspections play a crucial role in environmental conservation and resource management. However, these inspections traditionally depend on manual approaches, which are not only inefficient but also incur high costs. In response to this challenge, this study introduces an innovative drone-based approach to optimize offshore oilfield inspections, focusing specifically on minimizing the total flight duration through effective routing optimization. Based on this approach, we develop a novel and mathematical model that accounts for drone power limitations and inspection time windows. To solve this model efficiently, we propose a refined differential evolution algorithm. This algorithm incorporates both a roulette decoding method and a variable neighborhood search strategy, each contributing uniquely to enhance the solution quality. Experimental results demonstrate that our method markedly reduces the total flight duration of drones, substantially outperforming traditional approaches that do not incorporate routing optimization. This reduction in flight duration leads to more efficient and cost-effective drone operations for offshore oilfield inspections.

INDEX TERMS Offshore oilfield inspection, drone routing optimization, differential evolution, variable neighborhood search.

I. INTRODUCTION

In recent years, the development planning of offshore oil and gas fields has garnered substantial attention, spurred by the discovery of significant oil and gas reserves globally in the past decade [1]. However, the exploitation of offshore oilfields often entails the risk of marine oil spills, a major environmental concern. Such spills, being a primary source of water pollution, inflict extensive ecological and economic damages. They disrupt the marine ecosystem and adversely affect aquatic biodiversity [2]. Consequently, rigorous offshore oilfield inspection is an indispensable part of their exploitation process. Traditionally, these inspections have predominantly relied on manual boat patrols, a method suffering from markedly low efficiency. Addressing this inefficiency and enhancing the inspection process is thus a critical research challenge in the development of offshore oilfields. In parallel domains, drones equipped with mission-specific cameras and payloads have been employed for diverse purposes, such as powerline wear assessment, search and rescue operations, and fire surveillance [3]. This versatility underscores the potential of drones in offshore oilfield inspections. Accordingly, this study focuses on the offshore oilfield inspection planning with drone routing optimization (OOIPDRO), taking into account the power limitations of drones. By exploring this approach, the research aims to contribute to the efficiency and effectiveness of offshore oilfield inspections, proposing solutions that integrate advanced drone technology with strategic operational planning.

The remainder of this paper is organized as follows: Section II provides an overview of the related works pertaining to the OOIPDRO and highlights our significant contributions. Section III presents the formulation of the problem through a comprehensive mathematical model. Section IV elaborates on a heuristic algorithm developed for solving this complex problem. In Section V, we conduct and discuss a series of numerical experiments to validate the effectiveness of the proposed approach. Finally, Section VI concludes the paper with key findings and insights derived from this research.

The associate editor coordinating the review of this manuscript and approving it for publication was Bijoy Chand Chatterjee.

II. LITERATURE REVIEW

While the exploitation of offshore oilfields plays a pivotal role in global energy supply, the associated oil spills during operations pose severe threats to marine ecosystems. Magris and Giarrizzo highlighted that these spills resulted in extensive marine life mortality, damaged coral reefs and seabed ecosystems, and potentially induced long-term adverse effects on marine biodiversity [4]. Following the trend of marine ecosystem disruption, the infiltration of oil spill toxins into the food chain escalates the issue to a human health crisis, increasing cancer risks among other health problems [5]. Additionally, Câmara et al. underscored the significant economic impact on coastal economies, particularly fisheries and tourism, where oil spills could lead to billions in lost revenue [6]. In this context, efficient and timely inspections are paramount to preventing, detecting, and responding to oil spills. Zhang et al. advocated that effective monitoring and inspection strategies could identify potential oil spill risks early, enabling prompt intervention to avert disasters [7]. Such measures were also crucial in quickly responding to spills, mitigating environmental and economic impacts, and safeguarding marine and coastal community health. However, performing inspections in offshore oilfields is inherently challenging and complex. Shukla and Karki observed that their remote location far from major landmasses not only complicated access, increasing both difficulty and time, but also intensified the overall arduousness of the inspection process [8]. The unpredictability of the marine environment, including extreme weather conditions and strong currents, further escalated the challenges to inspector and equipment safety. Cheng et al. also highlighted the significant communication challenges encountered at sea [9]. Therefore, in light of these significant challenges, it becomes imperative to explore more efficient methods or approaches to conduct offshore oilfield inspection planning.

The rapid advancement of drone technology has established them as an efficient alternative for offshore oilfield inspections. Drones are characterized by their high flexibility, low operational costs, and ability to access remote or hazardous areas, addressing the critical needs of offshore oilfield inspections. In contrast to traditional manual boat patrols, drones offer quicker deployment and can cover larger areas, significantly enhancing the efficiency and effectiveness of offshore oilfield inspections. These attributes render drones particularly suitable for the challenging and complex environments of offshore oilfields. Drones equipped with high-resolution cameras capture detailed images, enhancing the precision of offshore oilfield inspections [10]. Their ability to gather comprehensive data is invaluable for oilfield operators. Furthermore, the rapid response capability of drones is crucial for timely identifying and reporting potential oil spills, aiding in prompt actions to mitigate environmental damage. Drones have been widely utilized in offshore and similar environments, showcasing their adaptability in a range of applications. Nooralishahi et al. conducted a comprehensive review of the evolving role of drones in non-destructive industrial inspections [11]. Chowdhury et al. examined drone usage in post-disaster scenarios, shedding light on their utility inefficient disaster management and assessment [12]. Siddiqui and Park demonstrated a drone-based system, combined with deep learning, for inspecting transmission line components [13]. Recent studies have also explored autonomous drone systems for electrical substation inspections [14], [15], [16]. In maritime inspection research, Shafiee et al. emphasized the application of drones in inspecting offshore wind turbines, a key component of advanced renewable energy maintenance [17]. The innovative use of drones in large-scale offshore wind farm inspections was further showcased in studies [18], [19], [20]. These examples demonstrated drones' potential in marine environment monitoring and offshore oilfield inspections, offering novel perspectives and methodologies. Despite the promising applications of drones in offshore oilfield inspections, the drone routing optimization, particularly under power constraints, often remains underexplored in existing literature.

Routing optimization plays a critical role in enhancing the efficiency of drone-based inspections, as it directly influences inspection completion time and resource utilization. Given the limited battery life and flight capability of most drones, optimizing their routes is essential to maximize the inspection area coverage within the shortest possible time, thereby elevating both the efficiency and quality of inspections. While routing optimization significantly enhances drone operational scope in inspections, existing research predominantly focuses on applications in last-mile logistics and emergency scenarios.

Significant research has been conducted on drone use for last-mile delivery, where drones serve either as a standalone mode of transport or in combination with other methods like trucks [21], [22], [23], [24], [25]. Another line of inquiry has focused on the deployment of drones, or drone-truck combinations, in emergency scenarios [26], [27], [28], [29], [30]. These studies have developed various mathematical models to optimize drone routing, offering solutions that consider technical, operational, and environmental factors in varying degrees of detail. However, the specific requirements of offshore oilfield inspections, such as the need to visit certain points multiple times within a given time window, present unique challenges not fully addressed in these studies. Furthermore, our research considers scenarios where drones return to base and depart multiple times, adding another layer of complexity to the drone routing optimization problem.

In summary, drone technology has evolved greatly in the realm of inspections, but its adoption for routing optimization in offshore oilfields lags behind. Presently, the majority of studies concentrate on examining the capabilities of drones in offshore environments, with an emphasis on their basic functionality and operational viability. However, these studies often overlook the critical role of drone routing optimization, a fundamental aspect in enhancing inspection efficiency

and reducing operational costs. Consequently, there is an imperative need to focus research efforts on drone routing optimization to fully harness the potential of drones in the context of offshore oilfield inspections. Below we summarize our contributions:

1) This study introduces an innovative approach to offshore oilfield inspection planning, utilizing drones with an emphasis on routing optimization to minimize energy costs. Compared to existing methods, this strategy enhances inspection efficiency, particularly by addressing the energy constraints of drones in long-duration and extensive area coverage tasks.
2) A comprehensive mathematical model accommodating multiple takeoffs by drones has been developed, incorporating various realistic constraints such as drone power limitations and inspection time windows. This model offers fresh insights and methodologies for tackling the complexities of maritime inspections.
3) To effectively address the NP-hard nature of the proposed model, this study designs an improved differential evolutionary algorithm. It features an innovative roulette decoding method to handle discrete problems and incorporates a variable neighborhood search (VNS) strategy for improved optimization performance. This algorithmic innovation goes beyond traditional problem-solving methods in the field, offering a more robust and efficient approach for tackling complex optimization challenges.

III. PROBLEM FORMULATION

A. PROBLEM DESCRIPTION

In maritime oilfield operations, drones have been increasingly adopted by inspection bases as a more efficient alternative to manual boat patrols for offshore site inspections. Over a planning period $|T|$, the base is tasked with dispatching $|K|$ drones to conduct multiple inspections at $|N|$ designated oilfield points. Unlike manual boats, a drone is constrained by a fixed safe flight duration Δ^{saf} due to battery constraints, ensuring each round trip from the base does not exceed this time limit. Additionally, each oilfield point requires regular inspections at an interval Δ^{int} within the planning period $|T|$, amounting to $|T|/\Delta^{int}$ inspections. Notably, if a drone arrives at the inspection point before the scheduled window opens, it must hover and wait to start the inspection at the designated time. Consequently, the core research problem of this study is to develop an optimal planning scheme for $|K|$ drones operating from a base to perform multiple inspections of $|N|$ oilfields. This scheme must adhere to the inspection time window constraints and consider the drones' safe flight duration, with the objective of minimizing the total flight duration for all drones.

Fig. 1 presents a detailed example of a drone scheduling scheme for offshore oilfield inspections. The illustration depicts four oilfield points requiring inspections, with each point scheduled for inspection twice within the planning period. Each inspection task is constrained by a specific

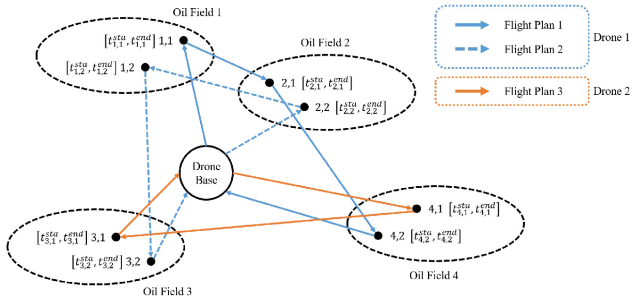

FIGURE 1. Example of offshore oilfield inspection planning with drones.

time window $[t_{n,m}^{sta}, t_{n,m}^{end}]$, indicating that inspections should occur within this period. In this example, drone 1 is tasked with two flight plans: the first covers inspection points [0]→[1,1]→[2,1]→[4,2]→[0]; the second involves [0]→[2,2]→ [1], [2]→[3,2]→[0]. Meanwhile, drone 2 is scheduled to follow a single flight plan, which includes [0]→[4,1]→[3,1]→[0]. To facilitate the model calculation, each inspection at every oilfield point is treated as a distinct pending visitation point denoted by i, included in the set P, where $|P|$ equals $|N||T|/\Delta^{int}$. Each pending visitation point i is also associated with its own inspection time window $[t_i^{sta}, t_i^{end}]$.

B. ASSUMPTIONS AND NOTATIONS

To optimize the drone-based inspection and scheduling in the offshore oilfield, and to maintain the model's scientific integrity, the following assumptions are made:

1) Each drone is fully charged upon every departure from the base.
2) Sufficient batteries are available at the base to guarantee immediate drone redeployment after return, with battery replacement time being negligible.
3) Offshore weather conditions permit drones to fly between points at a constant, safe speed.
4) Drones do not require additional time for on-site inspections at oilfield points.

Furthermore, Table 1 lists the notations used to formulate the model.

C. MODEL FORMULATION

Based on the notation defined in Table 1, the objective function of the integrated model can be expressed as follows:

$$\min f(H) = \sum_{k\in K}\sum_{r\in F} \alpha_{r,k}\,(\varepsilon_r - \tau_r) \tag{1}$$

The objective function (1) is designed to minimize the total flight duration required for drones to accomplish all planned inspections. This includes the hovering time when a drone arrives at an inspection point ahead of schedule.

1) CONSTRAINTS BETWEEN DRONES AND FLIGHT PLANS

$$\sum_{s\in F} \beta_{0,s}^{k} = 1 \forall k \in K \tag{2}$$

TABLE 1. Notations and descriptions.

Notation	Description
Inputs	
K	The set of drones, $k \in \{1, 2, \ldots, \lvert K \rvert\}$.
F	The set of drones' flight plans, $r, s, l \in \{1, 2, \ldots, \lvert F \rvert\}$.
P	The set of inspection points, $i, j, h \in \{1, 2, \ldots, \lvert P \rvert\}$.
Δ^{saf}	The safe time of drones.
$D_{i,j}$	The flight time for a drone flying from inspection point i to j.
$[t_i^{sta}, t_i^{end}]$	The time window of the inspection point i.
M	A large positive number.
Decision variables	
$\alpha_{r,k}$	1 if the flight plan r is assigned to drone k; 0 otherwise.
$\beta_{r,s}^k$	1 if the flight plan s immediately follows the flight plan r in the inspection schedule of drone k; 0 otherwise.
τ_r	The start time of the flight plan r.
ε_r	The end time of the flight plan r.
$a_{i,r}$	1 if the inspection point i is in the flight plan r.
$b_{i,j}^r$	1 if the inspection point j is the immediate next node to be inspected after the point i in the flight plan r; 0 otherwise.
u_i	The arrival time of the inspection point i.

$$\sum_{r \in F} \beta_{r,0}^k = 1 \forall k \in K \tag{3}$$

$$\sum_{r \in F+\{0\}} \beta_{r,l}^k = \sum_{s \in F+\{0\}} \beta_{l,s}^k = 1 \forall l \in F, k \in K \tag{4}$$

Constraints (2) to (4) establish the scheduling scheme for each drone k, detailing the sequence in which various flight plans are to be executed within the schedule. It should be noted that these constraints specify that only one flight plan can be undertaken by a drone in each phase.

$$\sum_{s \in F+\{0\}} \beta_{r,s}^k - \alpha_{r,k} = 0 \forall r \in F, k \in K \tag{5}$$

Constraint (5) delineates the interrelation between the variables β and α, a crucial aspect for facilitating the resolution of the objective function.

$$\varepsilon_r - \tau_r \leq \Delta^{saf} \forall r \in F \tag{6}$$

$$\tau_s - \varepsilon_r + M\left(1 - \beta_{r,s}^k\right) \geq 0 \; \forall r, s \in F, k \in K \tag{7}$$

Constraints (6) and (7) define the time window constraints for each flight plan. Constraint (6) stipulates that the total flight duration of each plan must not exceed the drone's safe flight duration. Constraint (7) mandates that the end time of each trip for a given drone k must precede the start time of its subsequent flight plan, thereby ensuring that each drone executes only one flight plan at any given moment.

2) CONSTRAINTS BETWEEN FLIGHT PLANS AND INSPECTION POINTS

$$\sum_{j \in P} b_{0,j}^r = 1 \forall r \in F \tag{8}$$

$$\sum_{i \in P} b_{i,0}^r = 1 \forall r \in F \tag{9}$$

$$\sum_{i \in P+\{0\}} b_{i,h}^r = \sum_{j \in P+\{0\}} b_{h,j}^r = 1 \forall h \in P, r \in F \tag{10}$$

Constraints (8) to (10) establish the inspection itinerary for each flight plan r, outlining the sequence in which various inspection points are to be visited. Constraints (8) and (9) ensure that each flight plan starts and ends at the base, respectively. Constraint (10) requires that only one node is visited in each phase of the flight plan.

$$\sum_{j \in P+\{0\}} b_{i,j}^r - a_{i,r} = 0 \forall i \in P, r \in F \tag{11}$$

$$\sum_{k \in K} \sum_{r \in F} \alpha_{r,k} a_{i,r} = 1 \forall i \in P \tag{12}$$

Constraint (11) defines the interrelation between variables β and α. Meanwhile, constraint (12) requires that all inspection points must be visited within the overall inspection planning.

$$u_j - u_i + M\left(1 - b_{i,j}^r\right) \geq D_{i,j} \forall i, j \in P, r \in F \tag{13}$$

$$u_j - \tau_r + M\left(1 - b_{0,j}^r\right) \geq D_{0,j} \forall j \in P, r \in F \tag{14}$$

$$\varepsilon_r - u_i + M\left(1 - b_{i,0}^r\right) \geq D_{i,0} \forall i \in P, r \in F \tag{15}$$

$$t_i^{sta} \leq u_i \leq t_i^{end} \; \forall i \in P \tag{16}$$

Constraints (13) to (15) dictate the time window requirements for the inspection points. Constraint (13) ensures that the flight time between any two points adheres to the safe flight duration. Constraints (14) and (15) are employed to calculate the start and end times of each flight plan, respectively. Lastly, constraint (16) stipulates that the drone's arrival at any inspection point i must fall within its designated time window $[t_i^{sta}, t_i^{end}]$. In cases where the drone arrives early, it is required to hover over point i, waiting until t_i^{sta} before proceeding to the next inspection point.

3) DOMAINS FOR THE DECISION VARIABLES

$$\alpha_{r,k}, \beta_{r,s}^k, a_{i,r}, b_{i,j}^r = \{0, 1\} \forall i, j \in P, r, s \in F, k \in K \tag{17}$$

$$\tau_r, \varepsilon_r, u_i \geq 0 \forall i \in P, r \in F \tag{18}$$

IV. SOLUTION METHOD

A. DE-VNS

The multi-drone routing optimization problem with time windows is classified as an NP-hard problem [12]. To effectively tackle this challenge, we develop an enhanced DE-VNS optimization algorithm, building upon the foundation of the differential evolution (DE) algorithm. The DE-VNS algorithm incorporates two significant improvements: firstly, a roulette-based encoding and decoding method tailored to the specifics of our mathematical model, addressing the limitations of the standard DE algorithm in handling discrete problems; and secondly, this enhanced approach integrates VNS optimization, which augments the depth exploration capability of the standard DE algorithm, thereby boosting its overall optimization performance. Fig. 2 illustrates a schematic overview of the solution method.

Our algorithm, rooted in the DE framework, commences with a random initialization method to generate the ini-

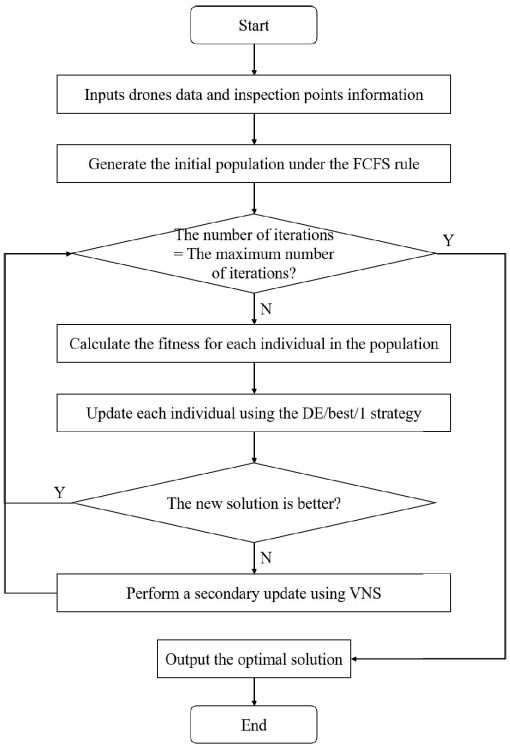

FIGURE 2. Overview of the DE-VNS.

tial solution population. This initial phase incorporates a roulette-based encoding and decoding strategy for individual solutions, detailed in Section IV.B. During each iteration loop, the fitness of each population member is evaluated, with the fitness calculation method outlined in Section IV.C. In the population update phase, individuals are first modified using the DE/BEST/1 strategy. Should this update be unsuccessful, VNS is then employed for local refinement, providing a secondary update operator. The specific VNS strategy employed is elaborated in Section IV.D. The algorithm ends once the iteration count is met or an early convergence is detected, at which point it outputs the optimal solution.

B. ROULETTE-BASED ENCODING AND DECODING

The standard DE algorithm is traditionally tailored for optimizing continuous variables, employing a real-number encoding mechanism. To address the limitation of the standard DE algorithm in dealing with discrete problems, we develop a roulette-based encoding and decoding method, specifically designed to align with the discrete nature of the problem addressed in this paper.

Our tailored DE algorithm still employs real-number coding, with the coding length dimension set to $|P|$. Each element's value lies within the range of $[1, |K|+1)$, where each element corresponds to a specific inspection point i. This setup reflects the number of drones, $|K|$, available for the offshore oilfield inspections. The decoding process unfolds in two steps: firstly, the integer part of the coding determines the drone assigned to each inspection point, allowing us to ascertain the set of points each drone is responsible for. Secondly, the flight plans are allocated based on the roulette wheel rule. To vividly demonstrate this encoding and decoding methodology, consider the following arithmetic example: with $|P| = 8$ inspection points and $|K| = 2$ drones, the encoding length is 8, and the range of values is $[1, 3)$. Given an initial encoding of [1.1, 1.19, 2.41, 2.27, 1.83, 1.77, 1.96, 1.24], the decoding process is illustrated in Fig. 3. This process can be detailed as follows:

1) Separate the integer and decimal parts of each code value. Inspection points with an integer part corresponding to 1 are assigned to drone 1, while those with an integer part of 2 are allocated to drone 2. Consequently, this yields the set of inspection points for drone 1 as {point 1, point 2, point 5, point 6, point 7, point 8}, and for drone 2 as {point 3, point 4}.
2) Determine the specific inspection planning for each drone, taking drone 1 as an example. Based on Step 1, drone 1's corresponding inspection points are {point 1, point 2, point 5, point 6, point 7, point 8}. These points can be divided into up to four trips, considering the drones' safe flight duration constraints in the problem. A roulette model is then constructed for drone 1, where the decimal part of each point's code dictates its flight plan allocation. Specifically, inspection points with decimal values in the interval $[0, 0.25)$ are assigned to flight plan 1; those in $[0.25, 0.5)$ to flight plan 2; in $[0.5, 0.75)$ to flight plan 3; and finally, those in $[0.75, 1)$ to flight plan 4. Within each flight plan, the inspection points are ordered in ascending sequence based on the decimal values of their codes, determining the visitation sequence. As a result, the first flight plan for drone 1 is $0\rightarrow1\rightarrow2\rightarrow8\rightarrow0$, while the second and third flight plans are empty, and the fourth is $0\rightarrow6\rightarrow5\rightarrow7\rightarrow0$. After removing empty flight plans, drone 1's final inspection planning is: $0\rightarrow1\rightarrow2\rightarrow8\rightarrow0$ (flight plan 1) and $0\rightarrow6\rightarrow5\rightarrow7\rightarrow0$ (flight plan 2). Drone 2, with its assigned points, has a single flight plan: $0\rightarrow4\rightarrow3\rightarrow0$, where '0' denotes the base and numbers 1-8 represent the inspection points.

C. FITNESS CALCULATION

The encoding and decoding method illustrated in Fig. 3 is not only succinct and effective but also straightforward to implement, enabling rapid and complete mapping between the encoded continuous variable space and the discrete problem's solution space. However, this encoding method does not directly account for the drone's safe flight duration constraints and the inspection time window constraints for each inspection point. To effectively address these complex constraints, we construct the fitness function $Fitness(H)$ utilizing a penalty mechanism to evaluate the scheduling scheme H.

$$\begin{aligned} &Fitness\,(H) \\ &= F\,(H) + \lambda^{d} \sum_{r\in F} \sum_{k\in K} \max\left\{0, \alpha_{r,k}\left(\varepsilon_r - \tau_r - \Delta^{saf}\right)\right\} \\ &\quad + \lambda^{p} \sum_{i\in P} \max\{0, u_i - t_i^{end}\} \end{aligned} \tag{19}$$

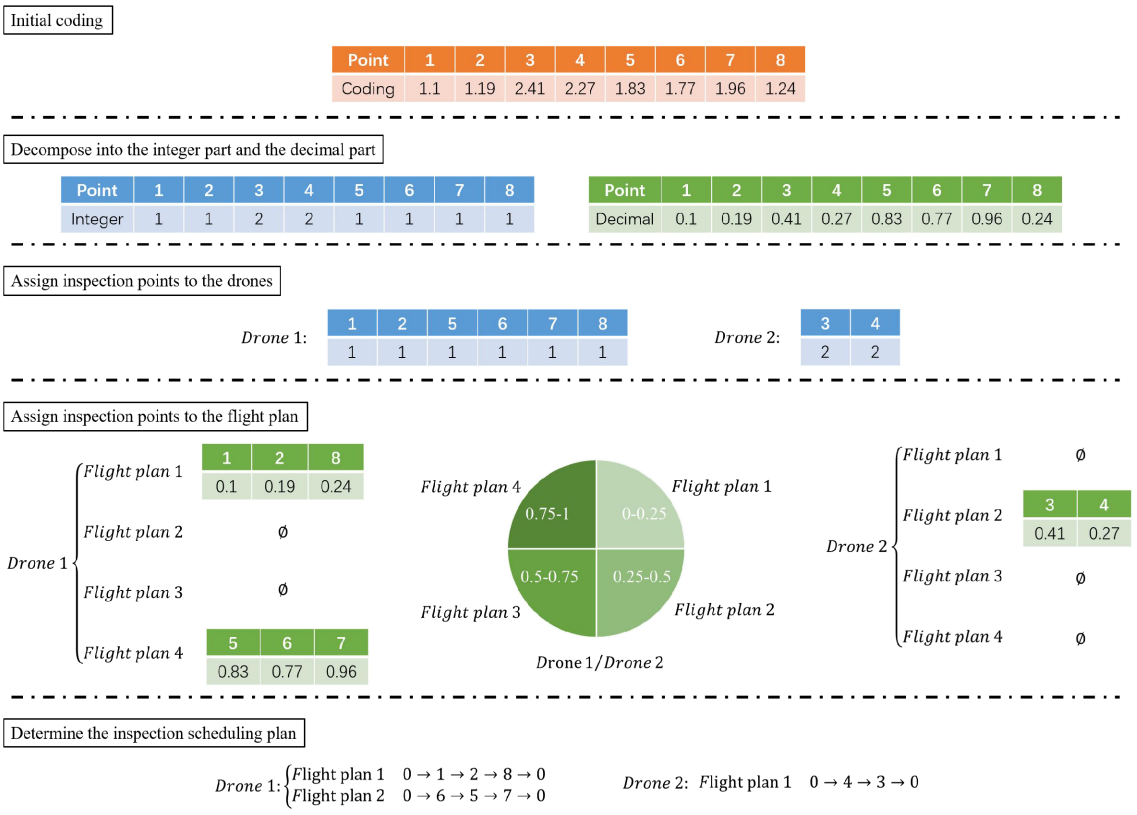

FIGURE 3. Overview of the DE-VNS.

Here, λ^d is the penalty factor applied for exceeding the safe flight duration Δ^{saf}, and λ^p is imposed when a drone's arrival time is later than the end time t_i^{end} of an inspection point.

D. VNS

To avoid the algorithm settling into a local optimum and to further improve its optimization capabilities, this study incorporates two VNS strategies tailored to the specific characteristics of the problem: the longest path update operator and the highest penalty time update operator.

1) The longest path operator is employed to update the flight plan with the longest path distance. This is achieved by conducting a neighborhood search aimed at finding a shorter flight distance. Fig. 4 illustrates the neighborhood search rule for this strategy. If flight path 1 has the longest distance in the current plan, it is targeted for optimization to reorder its inspection sequence towards a more efficient path. It should be noted that if flight path 1 is already optimized, then the operator targets the second longest path in the subsequent flight plan for updating.
2) The highest time penalty operator calculates each point's time penalty in the schedule, and then selects and updates the position of the point with the highest penalty. Fig. 5 demonstrates the neighborhood search rule for this strategy, focusing on minimizing the time penalty. In the current scenario, point 1 incurs the highest time penalty, prompting its relocation to a new position where it can achieve the lowest total time penalty in the existing schedule.

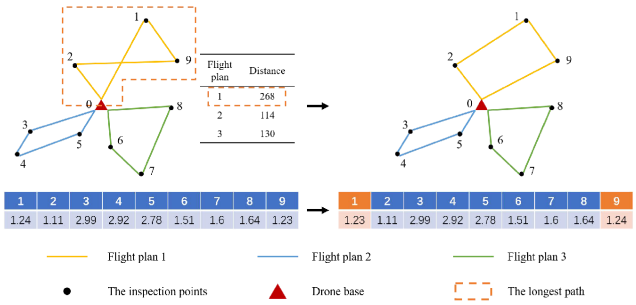

FIGURE 4. Schematic diagram of the longest path operator.

V. COMPUTATIONAL EXPERIMENTS

To validate the efficacy of our proposed model and solution method, we conducted a series of experiments on a computing server equipped with an Intel(R) Core(TM) i7-1065G7 CPU @ 1.30GHz, 1.50 GHz, and 16 GB RAM. The experimental framework is divided into three key segments: i) an experiment involving 6 oil fields and 2 drones; ii) an analysis of the

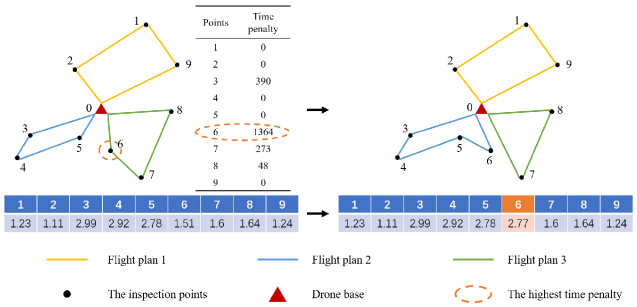

FIGURE 5. Schematic diagram of the highest time penalty operator.

effectiveness of our proposed scheme; and iii) an assessment of solution quality.

A. 6-OILFIELD AND 2-DRONE EXPERIMENT

For the target experiment, we designed a scenario with six oil field points and two drones within a daily operational cycle. In this scenario, each oil field requires inspection every two hours, cumulatively amounting to a total of 72 inspection points over a 24-hour period. The entire inspection region is defined within a 100×100 coordinate system, with the drone base located at coordinates (50,60). The positions of the six oilfield inspection points are randomly generated within this map, as depicted in Fig. 6.

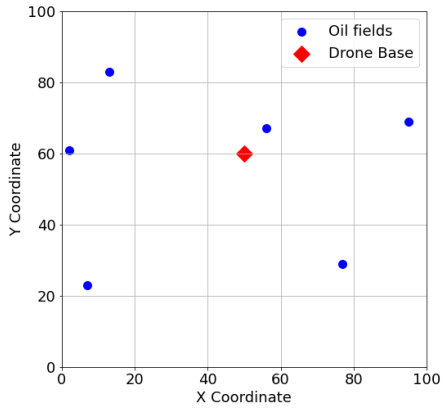

FIGURE 6. Layout of oilfields location.

Following the computation, the inspection planning was derived as detailed in Table 2. The cumulative flight duration for the two drones totaled 1703 minutes. Importantly, all inspection activities occurred within their respective time windows, and the total flight duration for each drone's flight plan adhered to the safe flight duration limits.

B. SCHEME EFFECTIVENESS: COMPARISON WITH THE FCFS APPROACH

In this subsection, we demonstrate the effectiveness of our optimization scheme in comparison with the First-Come-First-Serve (FCFS) approach. FCFS, a traditional method, selects oilfield inspection points based on the earliest service time windows for inspection, but it mainly focuses on the safe flight duration. Any exceedance of the time window is directly counted as a time penalty in the objective function. Table 3 shows the objective function comparison between FCFS and our scheme at different scales. Table 4 details the specific inspection planning differences under the 5-oilfield-2-drone example. It is evident that as the number of oilfield points and drones increases, our optimization scheme exhibits greater superiority. This advantage stems from FCFS's lack of consideration for drone routing optimization, resulting in fewer inspectable points within the safe flight duration for each drone's journey.

TABLE 2. Inspection schedule for 6-oil field and 2-drone experiment.

Drone	Flight Plan
Drone 1	0→6→1→4→3→0, 0→1→4→3→0, 0→5→2→5→6→0, 0→5→2→5→6→0, 0→2→5→2→6→0, 0→3→4→1→6→0, 0→1→4→3→0, 0→3→4→1→6→0, 0→3→4→1→0
Drone 2	0→2→5→2→6→0, 0→3→4→1→6→0, 0→1→4→3→0, 0→3→4→1→6→0, 0→3→4→1→0, 0→6→1→4→3→0, 0→1→4→3→0, 0→5→2→5→6→0, 0→5→2→5→6→0

C. SOLUTION QUALITY: COMPARISON WITH EXISTING METHODS

In this subsection, we conduct a comparative analysis between our DE-VNS algorithm and several prevalent algorithms in the field: GUROBI solver, Genetic Algorithm (GA), Artificial Bee Colony (ABC) algorithm, and Particle Swarm Optimization (PSO) algorithm. The comparative data results of these different algorithms across various scales are presented in Table 5. The parameter settings for these heuristic algorithms are as follows: i) DE-VNS: Maximum iterations set to 200, population size at 20, crossover probability at 0.2, and scaling factor at 0.2. ii) GA: Maximum iterations set to 200, population size at 20, crossover probability at 0.8, and mutation probability at 0.2. iii) ABC: Maximum iterations set to 200, with 20 employed bees, 20 onlooker bees, and 20 scout bees. The limit for the acceleration coefficient is set to 1, and the inertia weight damping ratio at 0.99. iv) PSO: Maximum iterations set to 200, population size at 20, maximum flight speed at 0.1, and weights at 1. The inertia weight damping ratio is set at 0.99, with an individual learning parameter of 1.5 and a global learning parameter of 2.

From the experimental data, it is evident that our algorithm's average deviation from GUROBI's results is a mere 1.32%. This modest deviation, coupled with the significantly faster solution processing of our heuristic algorithm compared to the commercial solver, demonstrates our algorithm's capability for efficiently finding the optimal inspection plan for the given problem. When contrasted with the other three heuristic algorithms, our algorithm shows an average deviation of 5.02% from GA, 12.86% from ABC, and 2.87% from PSO. This performance highlights not only the DE-VNS algorithm's ability to identify the optimal inspec-

TABLE 3. Comparison of the objective value obtained by the FCFS and our scheme.

Number of oil fields	Number of drones	Objective value		Confirm to time window		Gap
		DE-VNS	FCFS	DE-VNS	FCFS	
4	1	1411	1411	√	√	0.00%
4	2	1232	1411	√	√	14.53%
4	3	1232	1411	√	√	14.53%
5	1	1944	7340	√	×	277.57%
5	2	1752	5122	√	×	192.35%
5	3	1752	2578	√	√	47.15%
6	1	4192	8942	×	×	113.31%
6	2	1703	4743	√	×	178.51%
6	3	1536	2794	√	√	81.90%

TABLE 4. Comparison of the detailed inspection planning obtained by the FCFS and our scheme.

Scheme	Drone	Flight Plan
Our scheme	Drone 1	0→5→2→3→0, 0→1→5→2→0, 0→4→1→0, 0→4→3→0, 0→1→4→0, 0→4→3→0, 0→1→4→0, 0→3→4→0, 0→3→2→5→0, 0→2→5→1→0, 0→5→2→3→0, 0→2→5→1→0
	Drone 2	0→1→4→0, 0→3→4→0, 0→3→2→5→0, 0→2→5→1→0, 0→5→2→3→0, 0→2→5→1→0, 0→5→2→3→0, 0→1→5→2→0, 0→4→1→0, 0→4→3→0, 0→1→4→0, 0→4→3→0
FCFS	Drone 1	0→4→1→0, 0→4→5→0, 0→2→5→0, 0→3→1→0, 0→2→3→0, 0→1→4→0, 0→5→4→0, 0→2→5→0, 0→3→1→0, 0→2→3→0, 0→4→1→0, 0→4→5→0, 0→5→2→0, 0→1→3→0, 0→3→2→0
	Drone 2	0→2→5→0, 0→3→1→0, 0→2→3→0, 0→4→1→0, 0→4→5→0, 0→5→2→0, 0→1→3→0, 0→3→2→0, 0→4→1→0, 0→4→5→0, 0→2→5→0, 0→3→1→0, 0→2→3→0, 0→1→4→0, 0→5→4→0

TABLE 5. Comparison of DE-VNS, GUROBI solver, GA, ABC, and PSO.

Number of oil fields	Number of drones	Objective value					Gap			
		DE-VNS	GUROBI	GA	ABC	PSO	GUROBI	GA	ABC	PSO
4	1	1411	1401	1484	1600	1454	-0.71%	5.17%	13.39%	3.05%
4	2	1232	1232	1299	1394	1258	-0.00%	5.44%	13.15%	2.11%
4	3	1232	1226	1289	1389	1264	-0.49%	4.63%	12.74%	2.60%
5	1	1944	1933	2055	2208	2001	-0.57%	5.71%	13.58%	2.93%
5	2	1752	1736	1831	1981	1805	-0.91%	4.51%	13.07%	3.03%
5	3	1752	1752	1836	1968	1816	-0.00%	4.79%	12.33%	3.65%
6	1	4192	4015	4402	4723	4329	-4.22%	5.01%	12.67%	3.27%
6	2	1703	1655	1773	1912	1740	-2.82%	4.11%	12.27%	2.17%
6	3	1536	1503	1626	1729	1583	-2.15%	5.86%	12.57%	3.06%
Average		-	-	-	-	-	-1.32%	5.02%	12.86%	2.87%

tion plan but also its effectiveness in reducing flight costs by at least 2% compared to these other optimization algorithms.

VI. CONCLUSION

The primary objective of this study is to explore and optimize the application of drones in offshore oilfield inspections, with a specific emphasis on reducing the total flight duration of drones through effective routing optimization. We develop an innovative inspection planning that enhances inspection efficiency and addresses the battery constraints of drones in long-duration, wide-coverage missions. The key contributions of this research include the formulation of a mathematical model considering drone power limitations and inspection time windows, and the creation of an enhanced DE-VNS algorithm for solving this NP-hard problem. This algorithm uniquely integrates a roulette decoding method with a variable neighborhood search strategy, significantly boosting solution efficiency and offering novel approaches for complex optimization challenges.

However, the study is not without its limitations. One major constraint is the assumption of a fixed charging mode for drones, without considering variations in available flight time due to differing power levels, which may impact the model's accuracy and practical application. Additionally, our experimental design did not encompass all potential external factors that could influence the efficiency of drone inspections. Notably, elements such as varying weather conditions and the possibility of drone failures were not included in our scenario. These factors are crucial as they can significantly affect drone performance and, consequently, the generalization ability of the model in real-world settings. Future research should thus focus on optimizing drone charging and power management strategies, while also considering the dynamic impact of external factors such as weather conditions and drone reliability on flight capabilities and inspection efficiency. Addressing

these elements could enhance the model's robustness and applicability, leading to a more comprehensive understanding of drone-based offshore oilfield inspections.

In conclusion, this research provides fresh theoretical and practical insights into drone-based offshore oilfield inspection and routing optimization. While acknowledging its limitations, we anticipate that these findings will stimulate further research into drone power management and mission planning, contributing to the advancement of this field.

REFERENCES

[1] V. Gupta and I. E. Grossmann, "Offshore oilfield development planning under uncertainty and fiscal considerations," *Optim. Eng.*, vol. 18, no. 1, pp. 3–33, Mar. 2017, doi: 10.1007/s11081-016-9331-4.

[2] H. Singh, N. Bhardwaj, S. K. Arya, and M. Khatri, "Environmental impacts of oil spills and their remediation by magnetic nanomaterials," *Environ. Nanotechnol., Monitor. Manage.*, vol. 14, Dec. 2020, Art. no. 100305, doi: 10.1016/j.enmm.2020.100305.

[3] M. H. Frederiksen and M. P. Knudsen. (Apr. 2018). *Drones for Offshore and Maritime Missions: Opportunities and Barriers*. [Online]. Available: https://industriensfond.dk/wp-content/uploads/uniflip/1104464.pdf

[4] R. A. Magris and T. Giarrizzo, "Mysterious oil spill in the Atlantic Ocean threatens marine biodiversity and local people in Brazil," *Mar. Pollut. Bull.*, vol. 153, Apr. 2020, Art. no. 110961, doi: 10.1016/j.marpolbul.2020.110961.

[5] A. Ferguson, H. Solo-Gabriele, and K. Mena, "Assessment for oil spill chemicals: Current knowledge, data gaps, and uncertainties addressing human physical health risk," *Mar. Pollut. Bull.*, vol. 150, Jan. 2020, Art. no. 110746, doi: 10.1016/j.marpolbul.2019.110746.

[6] S. F. Câmara, F. R. Pinto, F. R. D. Silva, M. D. O. Soares, and T. M. De Paula, "Socioeconomic vulnerability of communities on the Brazilian coast to the largest oil spill (2019–2020) in tropical oceans," *Ocean Coastal Manage.*, vol. 202, Mar. 2021, Art. no. 105506, doi: 10.1016/j.ocecoaman.2020.105506.

[7] W. Zhang, C. Li, J. Chen, Z. Wan, Y. Shu, L. Song, L. Xu, and Z. Di, "Governance of global vessel-source marine oil spills: Characteristics and refreshed strategies," *Ocean Coastal Manage.*, vol. 213, Nov. 2021, Art. no. 105874, doi: 10.1016/j.ocecoaman.2021.105874.

[8] A. Shukla and H. Karki, "Application of robotics in offshore oil and gas industry— A review Part II," *Robot. Auto. Syst.*, vol. 75, pp. 508–524, Jan. 2016, doi: 10.1016/j.robot.2015.09.013.

[9] Z. Cheng, H. Wan, H. Niu, X. Qu, X. Ding, H. Peng, and Y. Zheng, "China offshore intelligent oilfield production monitoring system: Design and technical path forward for implementation," in *Proc. Abu Dhabi Int. Petroleum Exhib. Conf.*, Abu Dhabi, UAE, Oct. 2023, pp. 1–13, doi: 10.2118/216490-MS.

[10] K. E. Joyce, S. Duce, S. M. Leahy, J. Leon, and S. W. Maier, "Principles and practice of acquiring drone-based image data in marine environments," *Mar. Freshwater Res.*, vol. 70, no. 7, p. 952, 2019, doi: 10.1071/mf17380.

[11] P. Nooralishahi, C. Ibarra-Castanedo, S. Deane, F. López, S. Pant, M. Genest, N. P. Avdelidis, and X. P. V. Maldague, "Drone-based non-destructive inspection of industrial sites: A review and case studies," *Drones*, vol. 5, no. 4, p. 106, Sep. 2021, doi: 10.3390/drones5040106.

[12] S. Chowdhury, O. Shahvari, M. Marufuzzaman, X. Li, and L. Bian, "Drone routing and optimization for post-disaster inspection," *Comput. Ind. Eng.*, vol. 159, Sep. 2021, Art. no. 107495, doi: 10.1016/j.cie.2021.107495.

[13] Z. A. Siddiqui and U. Park, "A drone based transmission line components inspection system with deep learning technique," *Energies*, vol. 13, no. 13, p. 3348, Jun. 2020.

[14] H.-A. Langøker, H. Kjerkreit, C. L. Syversen, R. J. Moore, Ø. H. Holhjem, I. Jensen, A. Morrison, A. A. Transeth, O. Kvien, G. Berg, T. A. Olsen, A. Hatlestad, T. Negård, R. Broch, and J. E. Johnsen, "An autonomous drone-based system for inspection of electrical substations," *Int. J. Adv. Robotic Syst.*, vol. 18, no. 2, Mar. 2021, Art. no. 172988142110029, doi: 10.1177/17298814211002973.

[15] E. Ribeiro, A. C. M. Kanitz, M. A. I. Martins, K. D. Tomaz, and S. de Francisci, "Optimization of inspections of underground electricity distribution networks using UAV," in *Proc. 9th Int. Electr. Eng. Congr. (iEECON)*, Mar. 2021, pp. 89–92, doi: 10.1109/iEECON51072.2021.9440307.

[16] A. Prieto, I. Rodriguez, J. Rodas, E. Paiva, R. Gregor, E. Chaparro, and E. Prieto-Araujo, "Image processing technique applied to electrical substations based on drones with thermal vision for predictive maintenance," in *Proc. IEEE Int. Conf. Automat./25th Congr. Chilean Assoc. Autom. Control (ICA-ACCA)*, Oct. 2022, pp. 1–6, doi: 10.1109/ICA-ACCA56767.2022.10006138.

[17] M. Shafiee, Z. Zhou, L. Mei, F. Dinmohammadi, J. Karama, and D. Flynn, "Unmanned aerial drones for inspection of offshore wind turbines: A mission-critical failure analysis," *Robotics*, vol. 10, no. 1, p. 26, Feb. 2021, doi: 10.3390/robotics10010026.

[18] X. Huang, G. Wang, Y. Lu, and Z. Jia, "Study on a boat-assisted drone inspection scheme for the modern large-scale offshore wind farm," *IEEE Syst. J.*, vol. 17, no. 3, pp. 4509–4520, Sep. 2023, doi: 10.1109/JSYST.2023.3272948.

[19] K. Kabbabe Poleo, W. J. Crowther, and M. Barnes, "Estimating the impact of drone-based inspection on the levelised cost of electricity for offshore wind farms," *Results Eng.*, vol. 9, Mar. 2021, Art. no. 100201, doi: 10.1016/j.rineng.2021.100201.

[20] H.-M. Chung, S. Maharjan, Y. Zhang, F. Eliassen, and K. Strunz, "Placement and routing optimization for automated inspection with unmanned aerial vehicles: A study in offshore wind farm," *IEEE Trans. Ind. Informat.*, vol. 17, no. 5, pp. 3032–3043, May 2021, doi: 10.1109/TII.2020.3004816.

[21] N. Agatz, P. Bouman, and M. Schmidt, "Optimization approaches for the traveling salesman problem with drone," *Transp. Sci.*, vol. 52, no. 4, pp. 965–981, Aug. 2018, doi: 10.1287/trsc.2017.0791.

[22] P. Bouman, N. Agatz, and M. Schmidt, "Dynamic programming approaches for the traveling salesman problem with drone," *Networks*, vol. 72, no. 4, pp. 528–542, Dec. 2018, doi: 10.1002/net.21864.

[23] Z. Wang and J.-B. Sheu, "Vehicle routing problem with drones," *Transp. Res. B, Methodol.*, vol. 122, pp. 350–364, Apr. 2019, doi: 10.1016/j.trb.2019.03.005.

[24] R. J. Kuo, S.-H. Lu, P.-Y. Lai, and S. T. W. Mara, "Vehicle routing problem with drones considering time windows," *Expert Syst. Appl.*, vol. 191, Apr. 2022, Art. no. 116264, doi: 10.1016/j.eswa.2021.116264.

[25] L. Vu, D. M. Vu, and V. Nguyen, "The two-echelon routing problem with truck and drones," *Int. Trans. Oper. Res.*, vol. 29, no. 5, pp. 2968–2994, Sep. 2022, doi: 10.1111/itor.13052.

[26] S. Chowdhury, A. Emelogu, M. Marufuzzaman, S. G. Nurre, and L. Bian, "Drones for disaster response and relief operations: A continuous approximation model," *Int. J. Prod. Econ.*, vol. 188, pp. 167–184, Jun. 2017, doi: 10.1016/j.ijpe.2017.03.024.

[27] C. Qu, F. B. Sorbelli, R. Singh, P. Calyam, and S. K. Das, "Environmentally-aware and energy-efficient multi-drone coordination and networking for disaster response," *IEEE Trans. Netw. Service Manage.*, vol. 20, no. 2, pp. 1093–1109, Jun. 2023, doi: 10.1109/TNSM.2023.3243543.

[28] B. Rabta, C. Wankmüller, and G. Reiner, "A drone fleet model for last-mile distribution in disaster relief operations," *Int. J. Disaster Risk Reduction*, vol. 28, pp. 107–112, Jun. 2018, doi: 10.1016/j.ijdrr.2018.02.020.

[29] G. Zhang, N. Zhu, S. Ma, and J. Xia, "Humanitarian relief network assessment using collaborative truck-and-drone system," *Transp. Res. E, Logistics Transp. Rev.*, vol. 152, Aug. 2021, Art. no. 102417, doi: 10.1016/j.tre.2021.102417.

[30] B. Shang, C. Wu, Y. Hu, and J. Yang, "An algorithm of visual reconnaissance path planning for UAVs in complex spaces," *J. Comput. Inf. Syst.*, vol. 10, no. 19, pp. 1–10, Oct. 2014.

HAOYAN ZHANG is currently pursuing the B.Sc. degree in marine engineering with Dalian Maritime University. His research interests include drone routing optimization and marine engineering.